

Estimating Regions of Wireless Coexistence with Gaussian Process Surrogate Models

Jacob D. Rezac
RF Technology Division
National Institute of
Standards and Technology
Boulder, CO, USA
jacob.rezac@nist.gov

Noel C. Hess
Department of Electrical Engineering
University of Colorado-Denver
Denver, CO
noel.hess@ucdenver.edu

Jason B. Coder
RF Technology Division
National Institute of
Standards and Technology
Boulder, CO
jason.coder@nist.gov

Abstract—Simultaneous coexistence of multiple wireless communications systems sharing the same spectrum is critical for the success of modern and future communications. We develop a technique for estimating regions of wireless coexistence (RWC) – the transmission configurations of each of the wireless systems which permit coexistence – based on measurements of key performance indicators (KPIs) of those systems. In this article we focus on two-way coexistence tests, which aim to determine the impact each of the communications systems have on each other. The new technique is based on a Gaussian process surrogate model of the unknown transmission-configuration-to-KPI functions. We introduce a sequential design of experiments based on this surrogate model which is designed to reduce the number of measurements necessary to reach a highly-accurate estimate of a RWC. On an illustrative example, this technique reduces the average number of required measurements by over 40% compared to a baseline experimental design. Similar results are achieved for a measurement-informed simulation based on a coexistence test between an Bluetooth Low Energy device and an IEEE 802.11n Wi-Fi devices.

I. INTRODUCTION

The increased proliferation of wireless communications devices necessitates that device performance be robust to limited spectrum availability. While some spectrum sharing is already common, for example within the Industrial, Scientific, and Medical (ISM) band, newly-developed and future communications technologies will require devices to use spectrum even more efficiently [1], [2]. Designers and testers of these devices must understand how transmission configurations (e.g., transmission power or coding schemes) impact wireless coexistence between devices. This is particularly true under some use cases, say a medical or industrial setting, where dependable coexistence between devices can be a safety concern.

A wireless coexistence test assesses the performance of multiple coexisting wireless devices under a number of operating conditions. In the two-way wireless coexistence tests we consider here, key performance indicators (KPIs) of both

systems are monitored as a function of transmission configuration and coexistence is achieved when both KPIs surpass a use-defined threshold. This is unlike a one-way coexistence test, which typically focuses only on the behavior of one device under test. As an example in a Wi-Fi-Bluetooth coexistence scenario, packet error rate (PER) of the Bluetooth device could be measured alongside throughput of the Wi-Fi device as a function of changing Wi-Fi transmit power. The KPIs in this scenario are Bluetooth PER and Wi-Fi throughput and the changing transmission configuration is Bluetooth transmit power. Coexistence can also be defined with respect to user-experience or mission-defined KPIs, though the KPIs we consider here are dictated by ease of measurement. Detailed wireless coexistence test plans are described in [3] and one-way coexistence studies are described for example in [4], [5], [6], [7], [8], [9], [10].

Two-way coexistence tests, compared to their one-way counterparts, are significantly more complicated as detailed information about all systems operating in the deployment environment is necessary. Detailed information on the RF activity in a given deployment environment can be difficult to obtain; assumptions and approximations are often made. In a two-way coexistence test, one is concerned with how their device or system performs among others and what their device contributes back into the RF environment. From a modeling perspective, the goal is to identify cases, settings, or configurations where both (or all) systems in the deployment environment can successfully operate. To the best of our knowledge, this is the first work to attempt to identify a region of mutual coexistence and provide guidance for a subsequent set of measurements.

In this article, we discuss a framework for estimating the transmission configurations of each wireless system which allows for wireless coexistence with high confidence. We introduce a new method to describe the set of reliable transmission configurations, which we call the *region of wireless coexistence* (RWC). In the Bluetooth-Wi-Fi coexistence scenario described above, the RWC is the range of Wi-Fi transmit powers which lead to both KPIs satisfying some threshold.

A high-resolution estimate of the RWC could be obtained by densely sampling the space of possible transmission configura-

This work of J.D. Rezac and J.B. Coder is U.S. Government work and not protected by U.S. copyright.

N.C. Hess participated in this work while affiliated with the University of Colorado at Denver. He is now with the Raytheon Company.

rations and monitoring the resulting KPIs of each system, such a measurement is infeasible for all but the simplest situations. As such, we also propose a method for improving estimates of the RWC by adaptively selecting transmission configurations based on a small set of previously-collected coexistence data. This adaptive design of experiments (DOE) requires fewer measurements to estimate the RWC than an experiment design which is not designed with RWC estimation in mind.

We compliment the measurements taken in the wireless coexistence tests with a data-driven surrogate model described by a Gaussian process (GP). This is a well-studied technique from statistical learning theory for estimating the output of an unknown function from a small set of measurements of the function and from assumptions about how rapidly the function can change. Many important statistics of GP models, briefly described in Section II, are exact expressions. This simplifies the estimation of the RWC and the adaptive DOE.

Adaptive DOEs with GP surrogate models have been studied previously primarily in the context of maximizing an unknown function through measurements [11]. Less work has been done towards estimating regions where the unknown functions meet some threshold. Different approaches to this problem with GP surrogate models are described in [12], [13], [14], [15], [16] and references therein. In the wireless coexistence scenarios we consider here, there are two KPIs being monitored. This seemingly-small change requires modification to prior work, which are documented below in Section II-A. We continue in Section III by discussing adaptive DOEs for multiple KPI scenarios. In Section IV, two examples demonstrate the feasibility of our approach to wireless coexistence scenarios. We study two examples in that section, one based on measurements and the other based on simulation. In each example, we compare the newly-developed adaptive DOE to more commonly-used DOE. Compared to these older baseline techniques, the newly-developed adaptive DOE reduces the number of measurements required for highly-accurate estimates of RWCs by around 40%.

A. Regions of Coexistence

We model the $J > 0$ test measurements performed in a two-way wireless coexistence test as the measured values y_1 and y_2 such that

$$y_1(\mathbf{x}_j) = f_1(\mathbf{x}_j) + \epsilon_1(\mathbf{x}_j) \quad \text{and} \quad y_2(\mathbf{x}_j) = f_2(\mathbf{x}_j) + \epsilon_2(\mathbf{x}_j).$$

Here, f_1 and f_2 are functions describing the true KPIs for each of the wireless systems as a function of M -dimensional ($M > 0$) vectors $\mathbf{x}_j \in \mathbb{X}$ ($j = 1, \dots, J$), which describe different transmission configurations within the set of all possible configurations, denoted $\mathbb{X} \subseteq \mathbb{R}^M$, and $\epsilon_i \sim \mathcal{N}(0, \sigma_i^2(\mathbf{x}_j))$ are Gaussian random measurement error with variance σ_i^2 ($i = 1, 2$). In this article we will take $M = 1$ (Wi-Fi transmit power) but there is no need for such a restriction. While the KPIs themselves are likely to be related, we model the noise components ϵ_1 and ϵ_2 to be statistically independent.

The regions of coexistence between f_1 and f_2 are the input values such that these true KPIs satisfy some quantitative

criteria. The prototypical example we consider in this article is the set of $\mathbf{x} \in \mathbb{X}$ such that $f_1(\mathbf{x}) \geq \tau_1$ and $f_2(\mathbf{x}) \leq \tau_2$ for user-supplied $\tau_1, \tau_2 \in \mathbb{R}$. In other words, coexistence in this example occurs when one KPI exceeds some threshold while the other is below a threshold. Note that coexistence is more flexible than this prototypical example and we more generally define coexistence according to the transmission configurations so that the KPIs belong to user-defined sets. We denote these sets as $T_1, T_2 \subset \mathbb{R}$ and the regions of coexistence are thus formally defined as

$$\Gamma_{T_1, T_2} := \{x \in \mathbb{X} : f_1(\mathbf{x}) \in T_1, f_2(\mathbf{x}) \in T_2\}.$$

The prototypical example thus takes $T_1 = (-\infty, \tau_1]$ and $T_2 = [\tau_2, \infty)$.

In practice, the values y_1 and y_2 are only known at a small set of measured locations \mathbf{x}_j , $j = 1, \dots, J$. As such, the aim of this work is to find measurement-based estimates of the binary classifier $\eta(x) := \mathbb{1}_{\Gamma_{T_1, T_2}}(x)$ for all $x \in \mathbb{X}$ which equals 1 when $x \in \Gamma_{T_1, T_2}$ and is zero otherwise.

II. GAUSSIAN PROCESSES AND ESTIMATION OF RWCs

Surrogate modeling with GPs has a long history, particularly in the evaluation of time-consuming computer simulations [16]. GPs are non-parametric models on which a priori assumptions of a function's regularity can be flexibly encoded. In particular, if a function f is sampled from a GP, then it is a collection of random variables, any subset of which is distributed as a multivariate Gaussian random variable with known mean and covariance. GPs are characterized by a mean function, $\mu(\mathbf{x})$, and covariance function, $k(\mathbf{x}_1, \mathbf{x}_2)$, which play the roles of the mean vector and covariance matrix of a multivariate Gaussian random variable. The mean function encodes general trends of f while the covariance function encodes smoothness assumptions, typically by implicitly dictating properties of the derivatives of a function sampled from the GP. Such a GP is denoted by $f \sim \mathcal{GP}(\mu(\mathbf{x}), k(\mathbf{x}_1, \mathbf{x}_2))$. More information about GPs is available, for example, in [17] and the references therein.

Remark 1. *The reader may object that GPs are a poor model for KPIs of interest in wireless communications. Many KPIs are percentages, for example, and so bounded on $[0, 1]$. On the other hand, all GPs have infinite extent. While there are well-understood ways to combat this [17], we are not concerned by such a mismatch in this article because we are using GPs as a surrogate model: in particular, they quickly estimate RWCs and adaptively indicate through the surrogate model where new measurements ought to be performed to improve that estimate. In the application of interest presented here, then, GPs provide a trade-off of computational complexity and model fidelity.*

To estimate RWCs, we assume a GP model sufficiently describes the configuration-to-KPI functions $f_1(\mathbf{x})$ and $f_2(\mathbf{x})$ based on measurements of those functions and use a GP surrogate to model these functions. We denote the GP surrogate based on $n > 0$ measurements $\mathbb{X}_n := \{\mathbf{x}_j\}_{j=1}^n$ (denoted

$y_i^{(n)}$ by $f_i^{(n)} \sim \mathcal{GP}(\mu_i^{(n)}, k_i^{(n)})$, $i = 1, 2$. In this article, we consider the surrogate models to be statistically independent because the measurement noise, which introduces randomness into y_1 and y_2 , is also independent. Note that as GPs, these have closed-form expressions [17],

$$\mu_i^{(n)}(\mathbf{x}) := (\mathbf{k}_i^{(n)})^T \left(\mathbf{K}_i^{(n)} + \sigma_i^2 \mathbf{I} \right)^{-1} y_i^{(n)}$$

$$k_i^{(n)}(\mathbf{x}_1, \mathbf{x}_2) = k_i(\mathbf{x}_1, \mathbf{x}_2) - (\mathbf{k}_i^{(n)})^T \left(\mathbf{K}_i^{(n)} + \sigma_i \mathbf{I} \right)^{-1} \mathbf{k}_i^{(n)}(\mathbf{x})$$

where $\mathbf{k}_i^{(n)}(\mathbf{x}) := [k_i(\mathbf{x}_1, \mathbf{x}), k_i(\mathbf{x}_2, \mathbf{x}), \dots, k_i(\mathbf{x}_n, \mathbf{x})]^T$ and $\mathbf{K}_i^{(n)}$ is the $n \times n$ matrix with entries $[k_i(\mathbf{x}_i, \mathbf{x}_j)]_{i,j=1}^n$. Calculation of important properties (e.g., confidence intervals around the estimated function values) of the surrogate model is then straightforward from these formulas.

A. Estimation of RWCs with GPs

We use $f_1^{(n)}(x)$ and $f_2^{(n)}(x)$ to estimate $\eta(x)$, the characteristic function of Γ_{T_1, T_2} . To do this, we construct a binary estimator $\hat{\eta}(x)$ from the GP as the estimator which minimizes the average integrated mean square error (IMSE) $\mathbb{E} \left[\int_{\mathbb{X}} (\eta(x) - \hat{\eta}(x))^2 dx \right]$ (here and elsewhere, the expectation operator is taken with respect to all functions generated by the GP surrogate model). This type of estimator was used in, e.g., [16], to find areas where a GP is larger than some threshold. We follow a similar, but slightly generalized approach.

The binary nature of both $\eta(x)$ and $\hat{\eta}(x)$ allows their IMSE to be expressed as

$$\mathbb{E} \left[\int_{\mathbb{X}} (\eta(x) - \hat{\eta}(x))^2 dx \right] = \int_{\mathbb{X}} (\mathbb{P} \{ \eta(x) \neq \hat{\eta}(x) \}) dx, \quad (1)$$

which is the integrated probability of misclassification. Using similar logic as in [16], the probability of misclassification can be expressed by

$$\tau^{(n)}(\mathbf{x}) = p^{(n)}(\mathbf{x}) + (1 - 2p^{(n)}(\mathbf{x}))\hat{\eta}(\mathbf{x}),$$

where $p^{(n)}(\mathbf{x}) := \mathbb{P} \left\{ f_1^{(n)}(\mathbf{x}) \in T_1, f_2^{(n)}(\mathbf{x}) \in T_2 \mid \mathbb{X}_n \right\}$ is the probability that the estimates of $f_1^{(n)}$ and $f_2^{(n)}$ fall within the RWC, conditioned on the n measurements \mathbb{X}_n . The probability of misclassification, and hence (1), is minimized by $\hat{\eta}(\mathbf{x}) = \mathbb{1}_{p^{(n)}(\mathbf{x}) > 1/2}$. Since the surrogate models $f_1^{(n)}$ and $f_2^{(n)}$ are modeled as statistically independent, $p^{(n)}(\mathbf{x}) = p_1^{(n)}(\mathbf{x})p_2^{(n)}(\mathbf{x})$ where $p_i^{(n)}(\mathbf{x}) = \mathbb{P} \left\{ f_i^{(n)}(\mathbf{x}) \in T_i \mid \mathbb{X}_n \right\}$. Using the equality $\mathbb{1}_{p_i^{(n)}(\mathbf{x}) > 1/2} = \mathbb{1}_{\mu_i(\mathbf{x}) \in T_i}$, which holds for GPs, this provides the binary estimate to $\eta(\mathbf{x})$ which we use in this article,

$$\hat{\eta}(\mathbf{x}) = \mathbb{1}_{\mu_1^{(n)}(\mathbf{x}) \in T_1} \mathbb{1}_{\mu_2^{(n)}(\mathbf{x}) \in T_2}. \quad (2)$$

We remark for below that due to its binary nature, $\text{Var}(\hat{\eta} \mid \mathbb{X}^{(n)}) = \left(p_1^{(n)}(\mathbf{x})p_2^{(n)}(\mathbf{x}) \right) \left(1 - p_1^{(n)}(\mathbf{x})p_2^{(n)}(\mathbf{x}) \right)$.

III. ADAPTIVE DESIGN OF EXPERIMENTS

In this section, we develop a measurement scheme designed to reduce the number of measurements required to estimate the RWC in a wireless coexistence test. We reduce the number of required measurements by only measuring at locations that the GP surrogate model suggests there is even a small possibility of coexistence. As more measurements are performed and the surrogate models improve, the experimental design we propose becomes composed almost entirely of transmission configurations which lead to coexistence. As the examples in Section IV demonstrate, such a goal-oriented design leads to a more than 40% reduction in required measurements for estimating a RWC at a high accuracy level, as compared to a baseline experimental design, which samples evenly from all possible transmission configurations.

Design of experiments is a well-studied field for efficiently learning about and building models describing a measurand from well-selected measurements [18]. Unlike classical experimental design which decide on the measurements to perform before an experiment begins, adaptive and goal-oriented experimental designs take an iterative approach to choosing which measurements to take. One well-known adaptive DOE is a maximin design, which aims to find the measurement location so that the minimum distance between the new location and all measured points is largest. Indeed, given a set of measurements $\mathbb{X}^{(n)} = \{\mathbf{x}_j\}_{j=1}^n$, the adaptive maximin point is the solution to

$$\mathbf{x}^{(n+1)} = \arg \max_{\mathbf{x} \in \mathbb{X}} \left\{ \min_{\xi \in \mathbb{X}^{(n)}} \|\mathbf{x} - \xi\|_2^2 \right\},$$

where $\|\cdot\|_2^2$ is the standard Euclidean distance. This measurement scheme is described as space-filling because it efficiently fills the possible measurement configurations [19].

In contrast to the maximin scheme, we aim to improve efficiency of the coexistence measurement by limiting samples to locations where the surrogate model predicts plausible coexistence. Simultaneously, we want to sample at locations which improve IMSE of $\hat{\eta}$. Each of these goals is accomplished by relying on statistical properties of the GPs $f_1^{(n)}$ and $f_2^{(n)}$ in a way we describe below. Note, however, that in order for these statistical properties to be trustworthy, the GPs must be sufficiently-accurate approximations of the true functions f_1 and f_2 . Balancing between taking samples that improve the estimate of $\hat{\eta}$ according to current information about the GPs and taking samples that learn more information about the GPs, is referred to as the exploration-exploitation trade-off. It is the balance between *exploring* areas of the GPs that are known poorly and *exploiting* previous measurements in order to determine where to sample next and reduce the IMSE of $\hat{\eta}$.

To simplify exposition, we assume henceforth that $T_1 = (-\infty, \tau_1]$ and $T_2 = [\tau_2, \infty)$ for known $\tau_1, \tau_2 \in \mathbb{R}$. The first step of our three-step DOE is to locate regions of \mathbb{X} that have any possibility to be part of the RWC, according to what measurements have thus far shown. To do this, we rely on $\mathcal{Q}_i^{(n)} = \left[\mu_i^{(n)}(\mathbf{x}) - \sqrt{\beta^{(n)}}\sigma_i^{(n)}, \mu_i^{(n)}(\mathbf{x}) + \sqrt{\beta^{(n)}}\sigma_i^{(n)} \right]$, where $\beta^{(n)}$ is a user-selected parameter. These sets specify

Algorithm 1 Adaptive DOE for RWC Estimation

Input: Initial design $(\mathbb{X}^{(0)}, y_1(\mathbb{X}^{(0)}), y_2(\mathbb{X}^{(0)}))$; thresholds (τ_1, τ_2) ; stopping index N ; hyperparameter function $\beta^{(n)}$; initial GP priors $\mu_i(\mathbf{x}), k_i(\mathbf{x}_1, \mathbf{x}_2), i = 1, 2$

Output: Estimate of RWC $\hat{\eta}^{(N)}$; surrogate models $f_1^{(N)}, f_2^{(N)}$.

- 1: **for** $n \leq N$ **do**
- 2: Estimate $f_i^{(n)}, u_i^{(n)}, \ell_i^{(n)}$ ($i = 1, 2$), and $\hat{\eta}^{(n)}$ from current measurements
- 3: Determine Optimistic RWCs with (3)
- 4: Find Exploration-Exploitation Sample Locations with (4) and (5)
- 5: Find Sample to Reduce Uncertainty on $\hat{\eta}$ with (6)
- 6: Take new measurement

$$(\mathbf{x}^*, f_1(\mathbf{x}^*) + \epsilon_1(\mathbf{x}^*), f_2(\mathbf{x}^*) + \epsilon_2(\mathbf{x}^*))$$

7: **end for**

confidence regions in which the true functions f_1 and f_2 are likely to reside, particularly for large-enough $\beta^{(n)}$ and n . Denote $\mathcal{Q}_i^{(n)} := [\ell_i^{(n)}(\mathbf{x}), u_i^{(n)}(\mathbf{x})]$ as the lower and upper bound functions. We optimistically determine plausible RWC sets, denoted by $\mathcal{O}^{(n)}$, by finding the $x \in \mathbb{X}$ so that $\ell_i^{(n)}(\mathbf{x})$ or $u_i^{(n)}(\mathbf{x})$ satisfy the threshold criteria for coexistence. For the T_1 and T_2 used in this discussion,

$$\mathcal{O}^{(n)} = \left\{ \mathbf{x} \in \mathbb{X} \mid \ell_1^{(n)}(\mathbf{x}) < \tau_1 \text{ and } u_2^{(n)}(\mathbf{x}) > \tau_2 \right\}. \quad (3)$$

This type of optimistic sampling draws inspiration from, for example, [12], [14], [20]. Unlike those works, we further subsample to iteratively improve the IMSE of $\hat{\eta}$. In particular, once the optimistic RWCs are available, we subsample within them to find the transmission configurations that minimize the integrated probability that $\hat{\eta}$ is incorrect,

$$\mathbf{x}_m^* = \arg \min_{\mathbf{x} \in \mathcal{O}^{(n)}} \mathbb{E} \left[\int_{\mathbb{X}} \tau^{(n+1)}(\mathbf{x}) d\mu(\mathbf{x}) \mid \mathbf{x}^{(n+1)} = \mathbf{x} \right] \quad (4)$$

and find the maximin point within $\mathcal{O}^{(n)}$,

$$\mathbf{x}_s^* = \arg \max_{\mathbf{x} \in \mathcal{O}^{(n)}} \left\{ \min_{\xi \in \mathbb{X}^{(n)}} \|\mathbf{x} - \xi\|_2^2 \right\}. \quad (5)$$

Note that computationally, the calculation of \mathbf{x}_m^* requires some form of statistical sampling. We use a Gauss-Hermite quadrature here, similarly to [16].

These two sampling points must be balanced in order to simultaneously improve the estimates of η and improve estimates of f_1 and f_2 . The first of these goals is achieved by only sampling within $\hat{\eta}$ while the second goal is achieved by exploring enough of \mathbb{X} . This is exactly the exploration-exploitation trade-off. To choose between these possible mea-

surement locations, we find which one minimizes the expected integrated variance around $\hat{\eta}$,

$$\mathbf{x}^* = \arg \min_{\mathbf{x} \in \{\mathbf{x}_m^*, \mathbf{x}_s^*\}} \mathbb{E} \left[\int_{\mathbb{X}} \text{Var} \left(\hat{\eta}^{(n+1)}(\mathbf{x}) \right) d\mu(\mathbf{x}) \mid \mathbf{x}^{(n+1)} = \mathbf{x} \right]. \quad (6)$$

As before, we calculate the expectation in (6) with Gauss-Hermite quadrature. Pseudo-code for this adaptive DOE is available in Algorithm 1.

IV. EXAMPLES

We consider two examples in this section to demonstrate the method discussed above. In the first example, we compare the performance of the adaptive experimental design developed in Section III to the performance of an adaptive, but not goal-oriented, maximin design and a non-adaptive uniform design. In the second example, we demonstrate the method on data informed by Bluetooth-Wi-Fi coexistence tests, described below.

In order to assess the algorithms we developed above, we determine the number of measurements required for $\hat{\eta}(\mathbf{x})$ to reach a true positive rate (TPR) of 95% and simultaneous false positive rate (FPR) of 5%. These metrics, defined as $\text{TPR} = (\text{Number of True Positives}) / (\text{Total Positives Reported})$ and similarly for FPR, provide a simple way to assess the success of RWC estimation in an example with known solution.

The GP surrogate model for these examples uses the GPML Toolbox Version 4.2 [21] though any similar GP modeling package is likely to produce equivalent results. In each example, we use a squared exponential covariance function, with hyperparameters chosen to minimize the marginal likelihood, and begin each experiment with an initial design of 4 uniformly-distributed points.

A. Example Problem

The first example problem we consider is a one-dimensional problem whose analytical properties can be easily determined but which also demonstrates important properties of the adap-

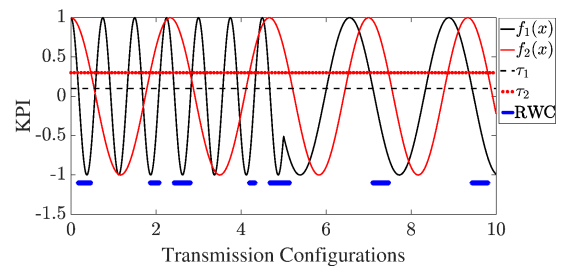


Fig. 1. The RWC (blue lines) and true functions (black and red lines) for the example in Section IV-A. Horizontal black and red dashes indicate the thresholds of interest for the simulations.

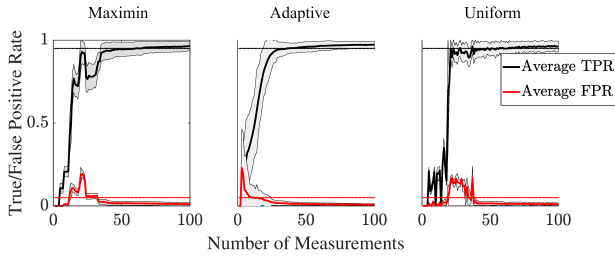


Fig. 2. Average TPR and FPR for three different sampling schemes: maximin (left), adaptive (middle), and uniform (right). Grey bars represent variability around mean. Horizontal lines at 0.05 and 0.95 represent the success metric for TPR and FPR.

tive experimental design discussed previously. In particular, we consider $\mathbb{X} = [0, 10]$ with functions

$$f_1(x) = \begin{cases} \cos(\omega_1 x) & x < c \\ (x - c - \cos(\omega_1 c)) \sin(\omega_1 + \pi/2 + \omega_2(x - c)) & x \geq c \end{cases}$$

$$f_2(x) = \cos(\omega_2 x)$$

representing the transmission-configuration-to-KPI functions with $\omega_1, \omega_2 > 0$, $c \in \mathbb{R}$. We use the sets $T_1 = (-\infty, 0.1]$ and $T_2 = [0.3, \infty)$ to determine coexistence. Although this coexistence scenario is contrived, it possesses challenging aspects for the estimation of the RWC and efficient sampling.

Fig.1 shows the true RWC for $\omega_1 = 8\pi/3$, $\omega_2 = 6\pi/7$, and $c = 5$. Notice that the RWC is the union of 7 sets of rather different size with gaps of varying size between them. A space-filling experimental design will inefficiently determine this RWC: an excessive amount of samples will be performed in locations which do not give any further information about the RWC.

To demonstrate the behavior of different sampling schemes, we performed 50 repeats of RWC estimation with different noise samples and compare sampling by a standard maximin scheme, by the adaptive DOE introduced above, and by non-adaptive uniform rectilinear sampling. The resulting TPR and FPR curves are indicated in Fig.2. Notice in particular that while the two space-filling designs quickly reach a TPR above 95%, this comes at the expense of a high FPR. The adaptive method introduced here is more balanced with respect to these

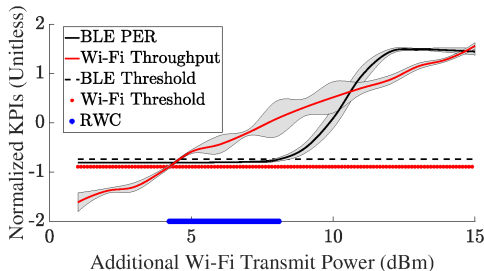


Fig. 3. Rescaled values of Bluetooth PER and Wi-Fi throughput as a function of additional Wi-Fi transmit power (dBm). Blue lines represent the RWC.

TABLE I

STATISTICS ABOUT THE NUMBER OF MEASUREMENTS REQUIRED TO REACH THE SUCCESS METRIC OF TPR > 0.95 AND FPR < 0.05 FOR THE EXAMPLE IN IV-A.

DOE	N	$\mathbb{E}(\hat{\eta}^{(q)})$	$\min_q(N[\hat{\eta}^{(q)}])$	$\max_q(N[\hat{\eta}^{(q)}])$
Maximin	61		35	> 100
Uniform	48		32	49
Adaptive	36		21	71

rates, and both TPR and FPR quickly reach their success thresholds without sacrificing the performance of the other metric.

Improved performance by the adaptive technique is further reflected in the reduction of measurements achieved by the adaptive scheme compared to the space-filling schemes: the adaptive DOE achieves a successful TPR and FPR metrics on average after 36 measurements, compared to the maximin scheme which meets this metric after 61 measurements (an improvement of nearly 41%) or the uniform scheme after 48 measurements (an improvement of 25%), both on average.

More complete statistics are available in Table I which additionally lists the best-case and worst-case experiments. Therein, $N[\eta]$ represents the first measurement so that TPR > 0.95 and FPR < 0.05 for a given RWC estimate η and $\hat{\eta}^{(q)}$, $q = 1, \dots, 50$, represents the RWC estimate for each repeat calculation. At most 100 measurements were allowed, so at times the maximin sampling scheme never reaches the desired threshold. Note that one repeat of the experiment resulted in a relatively high 71 measurements until success for the adaptive measurement scheme, demonstrating that there exist scenarios under which the new technique will occasionally perform worse than classical DOEs.

B. Experiment-Informed Example

This simulation emulates the behavior of a preliminary coexistence measurement test. This coexistence test tracked KPIs from two transceiving Bluetooth devices and two transceiving Wi-Fi devices which operated on the same frequency bands and were connected with coaxial cables to emulate user-designed coexistence and interference scenarios. The set of transmission configurations for this experiment was the transmission power of the transmitting Wi-Fi device and the KPIs-of-interest were the Bluetooth PER and Wi-Fi throughput. A description of a similar measurement campaign is available in [9], where a coexistence test was performed in a radiated fashion, rather than over coaxial cables.

The conducted test performed here included 10 repeat measurements of each KPI-of-interest over transmission conditions $\mathbb{X} = (1\text{dBm}, 2\text{dBm}, \dots, 15\text{dBm})$ as the Wi-Fi transmit power greater than a baseline transmit power¹. We define coexistence in this test as a Bluetooth PER below 3% and a Wi-Fi throughput above 43 Mbps. These values were chosen both

¹We express power in dBm as is common in wireless coexistence problems. This can be converted to milliwatts, the International System of Units standard unit of power, via $10^{\text{value in dBm}/10} \cdot 1\text{mW}$

as reasonable for this goal and to demonstrate the method. The data and threshold values were rescaled in this simulation to have zero mean and a standard deviation of 1.

We omit further details as this measurement campaign was used only to inspire a realistic simulation on which to demonstrate the techniques discussed above. Indeed, we define $f_1(x)$ by fitting a cubic spline through the average Bluetooth PER at each measurement location and $f_2(x)$ similarly for Wi-Fi throughput measurements. In the same way, we define each $\sigma_i(x)$ ($i = 1, 2$) by fitting a cubic spline through the standard deviation of the repeat measurements. This process gives an experiment-informed set of KPI functions, shown in Fig.3 on which to estimate the RWC, also shown in Fig.3. Note that, unlike in the previous example, the KPIs have non-uniform noise across \mathbb{X} , which we do not include as an a priori assumption in the GP surrogate model.

The true RWC in this example is sparse within \mathbb{X} , so we expect a space-filling design to inefficiently estimate the RWC. To demonstrate this, we performed again a simulation of 50 repeats of this coexistence experiment with different noise at each repeat shows that the adaptive DOE requires on average only 7.6 measurements to reach a TPR of 95% with FPR of 5%. A maximin scheme requires on average 12.24 so the adaptive measurement on average requires nearly 38% fewer measurements in this example.

V. CONCLUSIONS

We have developed a surrogate modeling technique for estimating the transmission configurations of two wireless systems, which allow them to coexist when sharing spectrum. The surrogate model leads to an efficient design of experiments for estimating such a RWC. While this technique shows promise on a simple coexistence example and an experimentally-driven example, there is the potential for significant improvement. For example, we have chosen hyperparameters heuristically in order to balance the exploration-exploitation trade-off. A theoretically-justified choice, such as the choice of β developed in [14], may lead to improvements.

We have focused here only on the case of a varying 1-dimensional parameter (transmission power) in the coexistence measurement. This is useful in many contexts, but we foresee that the techniques described here will be applicable in more complex coexistence scenarios. Indeed, the same techniques described above apply to estimating RWCs for parameters of multiple-dimension and we expect the adaptive technique proposed above to perform increasingly well as dimension grows due to the curse-of-dimensionality. Note, however, that GP surrogate models require significant computation resources for high-dimensional problems [17]. Higher-dimensional transmission configurations could include, for example, MAC-layer parameters of wireless devices.

In ongoing work, we are implementing these ideas on a similar BLE-Wi-Fi coexistence test with changing transmit powers from both the BLE and Wi-Fi devices able to change, compared to only the BLE discussed above. This will be a full two-way coexistence test on real test equipment. Finally, with

respect to potential improvements we point out [15] which solves a similar estimation problem by explicitly designing an adaptive measurement towards balancing true and false positives and negatives. This type of experimental design may lead to better outcomes in some wireless coexistence applications, particularly in wireless communications modalities that rely heavily on spectrum sharing.

REFERENCES

- [1] M. Shafi, A. Molisch, P. Smith, T. Haustein, P. Zhu, P. D. Silva, F. Tufvesson, A. Benjebbour, and G. Wunder, "5g: A tutorial overview of standards, trials, challenges, deployment, and practice," *IEEE Journal on Selected Areas in Communications*, vol. 35, pp. 1201–1221, 2017.
- [2] J. G. Andrews, S. Buzzi, W. Choi, S. V. Hanly, A. Lozano, A. C. K. Soong, and J. C. Zhang, "What will 5g be?" *IEEE Journal on Selected Areas in Communications*, vol. 32, pp. 1065–1082, 2014.
- [3] *Standard for Evaluation of Wireless Coexistence*, American National Standards Institute Std. C63.27, 2017.
- [4] M. Al Kalaa, S. Seidman, D. Witters, and H. Refai, "Practical aspects of wireless medical device coexistence testing," *IEEE Electromagnetic Compatibility Magazine*, vol. 6, no. 4, pp. 47–52, 2017.
- [5] M. Al Kalaa, S. Seidman, and H. Refai, "Estimating the likelihood of wireless coexistence using logistic regression: Emphasis on medical devices," *IEEE Transactions on Electromagnetic Compatibility*, vol. 60, no. 5, pp. 1546–1554, 2018.
- [6] M. Al Kalaa, J. Guag, and S. Seidman, "An outlook on wireless coexistence with focus on medical devices," *IEEE Electromagnetic Compatibility Magazine*, vol. 7, no. 3, 2018.
- [7] M. Al Kalaa and S. Seidman, "Wireless coexistence testing in the 5-GHz band with LTE-LAA signals," in *2019 IEEE International Symposium on Electromagnetic Compatibility, Signal & Power Integrity*, 2019, pp. 437–442.
- [8] —, "5-GHz band LTE-LAA signal selection for use as the unintended signal in ANSI C63.27 wireless coexistence testing," *IEEE Transactions on Electromagnetic Compatibility*, vol. 62, no. 4, pp. 1468–1476, 2020.
- [9] R. Jacobs, J. Coder, and N. J. LaSorte, "Verification of coexistence measurement methods: Radiated anechoic and open environment," in *2017 IEEE International Symposium on Electromagnetic Compatibility & Signal/Power Integrity*, 2017.
- [10] W. F. Young, J. Coder, and L. A. Gonzalez, "A review of wireless coexistence test methodologies," in *2015 IEEE Symposium on Electromagnetic Compatibility and Signal Integrity*, 2015, pp. 69–74.
- [11] J. Mockus, *Bayesian Approach to Global Optimization. Theory and Applications*. Dordrecht: Kluwer Academic, 1989.
- [12] B. Bryan, J. Schneider, R. Nichol, C. Miller, C. Genovese, and L. Wasserman, "Active learning for identifying function threshold boundaries," in *Proceedings of the 18th International Conference on Neural Information Processing Systems*, 2005, pp. 163–170.
- [13] R. Castro and R. Nowak, "Minimax bounds for active learning," *IEEE Transactions on Information Theory*, vol. 54, no. 5, pp. 2339–2353, 2008.
- [14] A. Gotovos, N. Casati, G. Hitz, and A. Krause, "Active learning for level set estimation," in *Proceedings of the Twenty-Third International Joint Conference on Artificial Intelligence*, 2013, pp. 1344–1350.
- [15] D. Azzimonti, D. Ginsbourger, C. Chevalier, J. Bect, and Y. Richet, "Adaptive design of experiments for conservative estimation of excursion sets," *Technometrics*, pp. 1–14, 2019.
- [16] J. Bect, D. Ginsbourger, L. Li, V. Picheny, and E. Vazquez, "Sequential design of computer experiments for the estimation of a probability of failure," *Statistics and Computing*, vol. 22, no. 3, pp. 773–793, 2012.
- [17] C. Rasmussen and K. Williams, *Gaussian Processes for Machine Learning*. Cambridge, Massachusetts: MIT Press, 2006.
- [18] D. Montgomery, *Design and Analysis of Experiments*, 10th ed. Wiley, 2019.
- [19] M. Tan, "Minimax designs for finite design regions," *Technometrics*, vol. 55, no. 3, pp. 346–358, 2013.
- [20] Y. Sui, A. Gotovos, J. Burdick, and A. Krause, "Safe exploration for optimization with gaussian processes," in *Proceedings of the 32nd International Conference on Machine Learning*, 2015.
- [21] C. Rasmussen and H. Nickisch, "Gaussian processes for machine learning (gpml) toolbox," *Journal of Machine Learning Research*, vol. 11, pp. 3011–3015, 2010.